Superparamagnetic Iron Oxide Nanoparticle Probes for Molecular Imaging

Daniel L. J. Thorek, Antony K. Chen, Julie Czupryna, and Andrew Tsourkas

Cellular and Molecular Imaging Group, Department of Bioengineering, University of Pennsylvania, Philadelphia, PA 19104

Abstract—The field of molecular imaging has recently seen rapid advances in the development of novel contrast agents and the implementation of insightful approaches to monitor biological processes non-invasively. In particular, superparamagnetic iron oxide nanoparticles (SPIO) have demonstrated their utility as an important tool for enhancing magnetic resonance contrast, allowing researchers to monitor not only anatomical changes, but physiological and molecular changes as well. Applications have ranged from detecting inflammatory diseases via the accumulation of non-targeted SPIO in infiltrating macrophages to the specific identification of cell surface markers expressed on tumors. In this article, we attempt to illustrate the broad utility of SPIO in molecular imaging, including some of the recent developments, such as the transformation of SPIO into an activatable probe termed the magnetic relaxation switch.

Keywords—Molecular imaging, Nanoparticles, SPIO, Magnetic resonance.

INTRODUCTION

The field of molecular imaging has recently gained widespread interest across a spectrum of disciplines. While it lacks a universal definition, molecular imaging can be outlined as the "non-invasive, quantitative, and repetitive imaging of targeted macromolecules and biological processes in living organisms."[57] The underlying premise of molecular imaging is that most disease processes can be identified by altered molecular profiles and/or cell behavior prior to visual anatomic alterations. Such insight could potentially allow for (1) the early detection of disease, (2) more accurate prognoses and personalized treatments, (3) the ability to monitor the effectiveness of therapeutic treatments, and (4) improvements in our understanding of how cells behave and interact in their intact environment in living subjects. Therefore, it is envisioned that molecular imaging could have a profound effect on progress in both the laboratory and the clinic.

Address correspondence to Andrew Tsourkas, Cellular and Molecular Imaging Group, Department of Bioengineering, University of Pennsylvania, 3320 Smith Walk, Philadelphia, PA 19104. Electronic mail: atsourk@seas.upenn.edu

In response to the promise of molecular imaging, the amalgamated field of bioengineering and nanotechnology has emerged to provide researchers and clinicians with a multiplying array of possibilities. The technology of magnetic nanoparticle probes, in particular, has seen increased efforts devoted to maturing its potential as a central tool for efficient, cross-application, molecular imaging. Although particles of iron oxide have been used as magnetic contrast agents for over 45 years,[46] refinement in the synthesis and coating of magnetic nanoparticles, especially in the last decade, has led to their employment in an abundance of novel biological applications. These applications include blood pooling, tissue and cell specific contrast agents for magnetic resonance (MR) imaging, cell tracking, and biomolecular detection.

Typically, magnetic nanoparticle probes for biomedical applications are comprised of nanoscale superparamagnetic iron oxide (SPIO) cores of magnetite and/or maghemite encased in polysaccharide, synthetic polymer, or monomer coatings. While other embodiments for MR contrast agents exist, including different transition metal systems such as cobalt-ferrite[97] or soluble paramagnetic chelates, such as gadolinium,[40,84] they are outside the scope of this review and will not be discussed in depth. Rather, this review will focus specifically on the use of SPIO as a molecular imaging agent. In particular, we will first discuss some of the physico-chemical properties and synthesis strategies of iron oxide nanoparticles. Then, we will provide an overview of the many exciting applications of SPIO both as a passive and active targeting imaging agent. Finally, we will examine several emerging applications for SPIO including cell tracking and magnetic relaxation switches.

PHYSICO-CHEMICAL PROPERTIES OF SPIO

Iron Oxide Core Structure

SPIO typically consist of two components, an iron oxide core and a hydrophilic coating. The SPIO core can be composed of magnetite (Fe_3O_4) and/or maghemite (γFe_2O_3). Maghemite is the ferrimagnetic cubic form of Fe(III) oxide

and it differs from the inverse spinel structure of magnetite through vacancies on the cation sublattice. However, both compositions possess similar lattice parameters at 8.396 and 8.346 Å for magnetite and maghemite, respectively.[14] Oxidation of synthesized SPIO converts Fe_3O_4 to γFe_2O_3 and can be accomplished through exposure to oxygen or oxidizing agents. This results in the change of the material appearance from a black-brown to a red-brown as Fe^{2+} in the magnetite lattice oxidizes. It should be noted, however, that the two iron oxide structures possess similar magnetic properties, although maghemite does have a slightly lower saturation magnetization.[25,141]

Classifications

SPIO sizes range greatly from 2 to 3 nm for citrate inhibited growth SPIO,[89] tens of nanometers for polymer-coated polycrystalline iron oxide nanoparticles through to micrometers for orally ingestible contrast agents. Larger diameters are available and are useful in such enterprises as cell tracking[134,58] and separation,[73] cell rheology and membrane deformation,[38,151] and as contrast agents for the gastrointestinal tract,[54] but have limited functionality in molecular imaging applications due to their limited accessibility to the neo- and microvasculature. Categories of SPIO, based on their overall diameter (including iron oxide core and hydrated coating), are noted in the literature[152] as oral-SPIO at between 300 nm and 3.5 μm; standard SPIO (SS-PIO) at approximately 60–150 nm; ultrasmall SPIO (US-PIO) of approximately 10–40 nm[156]; and monocrystalline iron oxide nanoparticles (MION—a subset of USPIO[34]) of approximately 10–30 nm.[135,158] MION nanoparticles are so named to underline the single crystal nature of their core. This is in contrast to SPIO greater than 50 nm that are comprised of multiple iron oxide crystals. Agents of all types excluding the MION category SPIO have either completed or are currently undergoing clinical testing (see Table 1). Generally speaking, all SPIO agents with less than a 50 nm diameter have been used for similar molecular imaging applications *in vivo*. Therefore, to avoid confusion, the term SPIO will be used to refer to all USPIO, MION, and CLIO (a form of MION with cross-linked dextran coating) for the remainder of this article.

Magnetism

The magnetic properties present in some ferromagnetic materials are the result of aligned unpaired electron spins. For these materials, magnetization is evident even in the absence of an external field. In a non-magnetized ferro-magnetic material, magnetic domains (so called Weiss-domains) at short range are aligned, but at long range adjacent domains are anti-aligned. The transition between these two domains is called a Bloch wall. At the nanometer scale ($\sim$14 nm), the formation of Bloch walls becomes thermodynamically unfavorable leading to the formation of single domain crystals, which are classified as super-paramagnetic.[35,137] The term superparamagnetic refers to the characteristic strong paramagnetic nature of the particles at this scale. Paramagnetic materials are distinguished through the tendency of their atomic magnetic dipoles to align with an external magnetic field, their small positive magnetic susceptibility (i.e., ability to strengthen the field they are in), and their random orientation in the absence of a magnetic field (due to Brownian fluctuations). SPIO have much larger susceptibilities (compared with strictly paramagnetic materials) as the entire crystal aligns with the applied field due to its single crystal nature.

When SPIO are placed in an external magnetic field their moments align in the direction of the magnetic field and enhance the magnetic flux. This ability to elicit substantial disturbances in the local magnetic field through large magnetic moments leads to a rapid dephasing of surrounding protons, generating a detectable change in the MR signal. Thus, the imaging capability provided is not from the SPIO intrinsically, but through their influence on longitudinal and transverse relaxation of the surrounding nuclei. Although the ability of SPIO to significantly reduce the spin–spin relaxation (T2) time is generally relied on for generating MR contrast,[68,99] it has also been demonstrated that SPIO can generate sufficient T1 contrast for biomedical applications as well; SPIO possess both high R1 and R2 relaxivities.[118,127] Upon removal of the magnetic field, Brownian motion is sufficient to randomize the SPIO orientations leaving no magnetic remanence. Brownian forces also prevent the aggregation of the SPIO due to magnetic attraction in solution.[123]

SPIO SYNTHESIS

There are several methods that are generally used to produce magnetic iron oxide nanoparticles, described in a rich patent and journal literature. Historically, long-term grinding of bulk magnetite in the presence of stabilizing surfactant produced the first documented ferrofluid.[103] Such mechanogrinding regimes are inherently time consuming and expensive. Currently, perhaps the most commonly accepted approaches for creating SPIO for biomedical applications concentrate around coprecipitation and microemulsion methods, although numerous other approaches are becoming more prevalent as the synthesis of SPIO with uniform core diameters becomes more desirable.

Coprecipitation

The most common method for production of magnetic nanoparticle populations involves synthesis via the coprecipitation of ferrous and ferric salts in an alkaline medium.[87,88,92,93,121] This synthesis approach can be conducted either in the absence or presence of surface complexing agents, such as dextran, polyethylene glycol (PEG), or

Table 1. Examples and properties of commercial SPIO agents (updated from Wang,[152]).

Agent	Class	Trade and common names	Status	Mean particle size
AMI-121	Oral SPIO	Lumirem, Gastromark, Ferumoxsil	Approved	>300 nm
OMP	Oral SPIO	Abdoscan	Approved	3.5 μm
AMI-25	SSPIO	Feridex, Endorem, Ferumoxide	Approved	80–150 nm
SHU555A	SSPIO	Resovist	Phase III	62 nm
AMI-227	USPIO	Sinerem, Combidex, Ferumoxtran	Phase III	20–40 nm
NC100150	USPIO	Clariscan	Completed phase II (discontinued)	20 nm
CODE 7228	USPIO	(Advanced magnetics)	Phase II	18–20 nm

polyvinyl alcohol (PVA). Surface complexing agents are often used to provide colloid stability and biocompatibility. Several SPIO-surface complexation agents are listed in Table 2.

Bare SPIO (i.e., without surface complexing agents) are created following the addition of a concentrated base to a di- and trivalent ferrous salt solution.[13] The precipitate is isolated through magnetic decantation or centrifugation. The precipitate is then treated with nitric or perchloric acid, centrifuged and peptized (i.e., colloidally dispersed) in water. This produces an acidic magnetic sol. Likewise, alkaline magnetic sols can be made using tetramethylammonium in place of the perchloric or nitric acid.[87] These magnetite nanoparticles are polydisperse with a mean diameter of approximately 10 nm and are roughly spherical in shape.[13]

Bare SPIO can subsequently be coated in monomers and polymers (Table 2) through non-specific adsorption following their purification to make them more suited for biomedical applications.[109] Alternatively, the monomers and polymers may be grafted to the nanoparticles during the precipitation step, although this will change the physical characteristics of the resulting nanoparticles.[13,32]

One commonly used coating for bare SPIO is silica. An advantage of coating contrast agents with silica is that one is able to tap the established database for silica surface modification.[114] The degree of silica-coating can be controlled,[11] resulting in coverage thickness between 2 and 100 nm.[85] The hydroxyl surface groups can be modified to display functional amines and carboxyls, relevant for further bioconjugation[56] and the silica itself can be dye-doped.[85,114]

As mentioned earlier, SPIO can also be formed directly in the presence of a coating polymer, usually dextran,[93,156] although a variety of coating systems are available (Table 2).[92,102] As with the bare SPIO, alkaline agents are used to coprecipitate the di- and trivalent ferrous salts, but here these salts have been dissolved directly in the presence of dextran.[92] The mean hydrodynamic radii of the polydisperse polymer-coated SPIO typically vary from ∼20 to above 100 nm (this can be controlled by adjusting synthesis parameters such as the dextran-to-iron ratio), while the iron oxide core size typically ranges from ∼2 to 15 nm.[135] Improved stability, including at elevated temperatures, can be imparted to the nanoparticles through an assortment of chemical modifications. The use of carboxymethyl reduced dextran[50] or cross-linking of surface adsorbed filaments with agents such as epichlorohydrin,[60,102] are just two examples of many. An important enhancement of polymer-coated SPIO for molecular imaging is their increased circulation lifetime[95] *in vivo* as the coating avoids the quick opsonization suffered by bare nanoparticles.[100]

Table 2. Common surface coatings and complexation agents.

Coating material	Advantages	References
Citric, gluconic, oleic	Larger SPIO core with thin organophillic coating	39, 48, 150
Dextran	Long plasma half-life, modifications	4, 92, 102, 153
Polycarboxymethyl dextran	Long plasma half-life, reduced diameter	50
Polyvinyl alcohol	Longer plasma half-life	92, 109
Starches	Wide pH stability, biocompatibility, availability, modifications	74
PMMA	Magnetic drug delivery vehicle	161
PLGA	FDA approved biocompatible coating	79
PAM	Multiple particle enmeshing matrix	91
PEG	Long plasma half-life, chemical modifications	53, 126, 162
PEG-lipid	Thin coating, available bioconjugation	101
Silane	Reactive to alcohol and silane coupling agents	18, 136
Silica	Inert, biocompatible coating	32

A wide variety of factors can be adjusted in the synthesis of the iron oxide nanoparticles in order to control size, magnetic characteristics, stability in solution, surface properties, and coatings leaving the synthesis of nanoparticles as more of an art than a science. The ionic strength and pH of the coprecipitation solution can be adjusted to control nanoparticle size over an order of magnitude (2–15 nm).[66] In addition, adjustment of the Fe(III)–Fe(II) ratios, heating regimes, and the dextran–iron ratios can be used to further control SPIO core size and overall hydrodynamic radius.[102,153] Although coprecipitation methods are widely utilized due to their simplicity and ability to be scaled up for large-scale reactions, the nanoparticles produced are fairly polydisperse. As a result, numerous other methods are currently being developed to make nanoparticles with more uniform dimensions.

Microemulsion

Microemulsions (oil-in-water and water-in-oil) have recently been adopted as nano-reactors for the synthesis of SPIO due to the ability to control the size and shape of the nanoparticles.[111] In general, nanoparticles are synthesized in oil-in-water microemulsions by suspending a ferrous salt-surfactant precipitate to an aqueous solution. A base (e.g., methylamine) is then added to form a magnetic precipitate. The size of nonstoichiometric mixed cobalt–zinc ferrite nanoparticles was found to depend on the presence of cobalt in the lattice.[59] In another embodiment, surfactant-(oleic acid) coated nanoparticles were added to a solution composed of a melted lipophilic suspension and an aqueous phase. This warm transparent phase when dispersed in cold water accomplished lipid coating of the colloidal magnetite.[63]

The water-in-oil approach is a more common microemulsion synthesis technique for nanoparticles with biomedical applicability. Strategies typically involve enclosing "nanodroplets" of aqueous iron salts in a surfactant coat that separates them from the surrounding organic solution (e.g., AOT in isooctane); to form reverse micelles.[29,113,132] To this, alkaline nanodroplets are added. The SPIO are precipitated and oxidized within the nano-sized micelle. Using variable reaction temperatures results in SPIO with diameters of 3–12 nm. Metal concentration and base concentration can also be used to vary nanoparticle size.[112]

Microemulsions are an efficient way to manufacture nanoparticles since the size of the microcavities formed can be tightly controlled between ∼2 and 12 nm.[111] Thus, this approach results in fairly uniform populations of SPIO. Although some microemulsion approaches produce nanoparticles that are only soluble in organic solvents,[78] these SPIO can be given water-soluble coatings that prevent agglomeration.[101] It should be noted that while it is generally accepted that microemulsion can produce SPIO with homogeneous sizes, this is dependent on the approach and precision. Further, microemulsion techniques have been criticized as an approach for synthesizing larger nanoparticles due to the formation of SPIO with poor crystallinity.[10]

Additional Methods

Numerous additional methods also exist for the controlled synthesis of SPIO including ultrasound irradiation and spray and laser pyrolysis. During ultrasound irradiation (also referred to as sonochemical synthesis), the rapid collapse of sonically generated cavities provides nanosecond lifetime hot spots of ∼5000 K where ferrous salts are instantly driven to form SPIO nanoparticles. Stabilization through oleic acid allows for the production of a monodispersed nanocolloid of ∼8 nm.[139] Using aerosol manufacturing techniques, such as spray and laser pyrolysis, continuous high-production rate formation of nanoparticles can be accomplished. In spray pyrolysis, a solution is sprayed into a series of reactors where the solute condenses as the solvent evaporates. Here, ferric ions are reduced to a mixture of ferric and ferrous ions in an organic compound, leading to SPIO formation.[20] A microporous solid is then sintered to a particle at high temperature. Laser pyrolysis can be used to reduce the reaction volume, as a laser heats a gaseous mixture of iron pentacarbonyl and air, producing nuclei that lead to small nanoparticles.[147] Uniform and well-crystallized nanoparticles are synthesized in a single step.[98] The high production rates of these methods come at the cost exhaustive control over experimental conditions and expensive equipment.

Recently, a method has been developed to synthesize high-quality SPIO by thermal decomposition of different iron precursors. Alivisatos' group have used FeCup3 in octylamine and trioctylamine at 250–300°C to form a monodisperse precipitate of maghemite.[122] Work is ongoing towards increasing the utility of thermally decomposed nanoparticles for biomedical applications[81]; specifically, to overcome their required suspension in organic solvents. Finally, another synthesis route is layer-by-layer (LBL) self-assembly, based on repeated submersion of a substrate or colloidal template in solutions of oppositely charged polyelectrolytes.[28] Stepwise adsorption of ions allows cores of nanoparticles or shells around existing particles to form. Although the large size of the particles may remain a limitation, Caruso *et al.* have developed protocols for dense and hollow SPIO sub-micron particles with interesting properties.[21,22]

BIOCOMPATIBILITY

The diameter and surface characteristics of the SPIO contrast agents are of importance in terms of clearance, cell response, and toxicity. In general, the spleen and liver as a result of mechanical filtration sequester SPIO above

approximately 200 nm in diameter. Particles below 10 nm are removed rapidly through extravasation and renal clearance.[53] In order to prolong plasma half-life, amphiphilic coatings are preferred, extending the circulation time of the particulates from minutes to hours,[104] thereby increasing the targeting capabilities of the contrast agent.

To date, studies have shown that the polymer-coated nanoparticles have minimal impact on cell viability and function. After incubation with immortalized fibroblasts, PEG-coated SPIO nanoparticles did not affect cell adhesion behavior or morphology.[52] Similarly, dextran-coated SPIO labeled with the Tat-internalizing peptide showed no significant effects on cell viability, clonogenic efficiency, immunophenotypic changes, or biodistribution for human hematopoietic cells.[80] Nonetheless, studies have shown that SPIO surface properties can influence the uptake of nanoparticles by phagocytic cells. For example, carboxydextran-coated SPIO (of equal or even smaller sizes) appear to be internalized by macrophages to a greater extent than dextran-coated SPIO.[90] It should be noted, however, that uptake of SPIO by macrophages is not associated with cell activation as no interleukine-1 release is observed.[116]

When used as a contrast agent in living subjects, adverse events from USPIO (dextran-coated SPIO) were noted as not serious, mild in severity, and short in duration.[3] The most common reactions were headache, back pain, vasodilatation, and hives. Magnetite biocompatibility has already been proven.[131,159] Following internalization, SPIO generally accumulate in lysosomes where the iron oxide core is broken down to iron ions through low pH exposure and these ions are incorporated into the hemoglobin pool.[154] Intracellular dextranase further assist with the degradation process by cleaving the dextran moiety. The use of dextran–iron complexes *in vivo*, stretches back over half a century, initially as a means to treat anemia.[41,83] Originally, dextran-coated iron oxide was developed to substitute for the ferritin iron complex, as a means to intravenously administer iron. The low toxicity of these agents over soluble iron salts translates into higher injectable concentrations of iron by as much as two orders of magnitude.[51]

PASSIVE TARGETING

SPIO probes lacking explicit molecular specificity are well known in the literature for imaging of biological systems via naturally directed physiological process. These include non-targeted cellular uptake, enhanced retention in tumors, macrophage phagocytosis, as well as accumulation in the liver, spleen, and lymph nodes. T2-weighted images reveal the presence of the SPIO through the T2 relaxation shortening effect resulting from the accumulation of nanoparticles. Propinquity of SPIO agents is a critical factor in enhancing the T2 relaxation effect,[140] as accumulation

of nanoparticles leads to more efficient transverse spin dephasing of water protons.[17,47] Perhaps most important for passive targeting is the hydrodynamic radius and the surface charge of the SPIO (factors related to the SPIO coating material), as these parameters control the circulation time of the nanoparticles, accessibility to tissues, opsonization, and rate of cell-type uptake.

Liver and Splenic Imaging

It has been demonstrated that larger nanoparticles (~150 nm hydrodynamic radius) such as the dextran-coated SSPIO AMI-25 are non-specifically taken up by Kupffer cells in the healthy liver, allowing for hepatic imaging. Further, the absence of Kupffer cells in malignancies has been exploited to allow for enhanced accuracy in discerning between healthy and diseased tissue through SPIO endowed contrast.[117,133,149] In addition to the detection and characterization of liver lesions, larger nanoparticles such as SHU555A and AMI-25 have also been shown capable of detecting focal splenic tumors.[5,157,160] Reimer *et al*., in imaging hepatic lesions, clearly show the power of enhanced detection through the use of SPIO,[117] (Fig. 1).

Lymph Node Imaging

In contrast to SSPIO, smaller iron oxide nanoparticles (~30 nm hydrodynamic radius) are found to accumulate in lymph nodes.[82,86,95,155] Specifically, the SPIO extravasate from the vasculature to the interstitial space where they are transported to the lymph nodes via the lymphatic vessels. The absence of SPIO in lymph nodes as determined by MR imaging has been shown to correlate with disturbances in lymph node flow or architecture due to the presence of metastases. The T2 shortening due to SPIO accumulation was pronounced in normal nodes, allowing for significant increases in positive predictive values and accuracy of diagnosis of node metastases[3] (Fig. 2). Thus, while lacking molecular targeting specificity, these agents have been used to discern between metastatic and inflammatory tumors through MR imaging.[4,55]

Cancer Imaging

Numerous studies have shown that in addition to detecting lymph node metastases SPIO can also be used to detect solid tumors directly. It has been found that SPIO passively accumulate at the tumor site due to the presence of leaky vasculature as well as from macrophage uptake.[95,116,165] The extent of tumor extravasation depends on the porosity of the angiogenic tumor vessels.

Enhanced detection of bone marrow is possible through SPIO[27,61] and possibly SSPIO, such as AMI-25 as well.[146] Bone marrow lesions are usually detected with high sensitivity, except in the complicating cases of children and
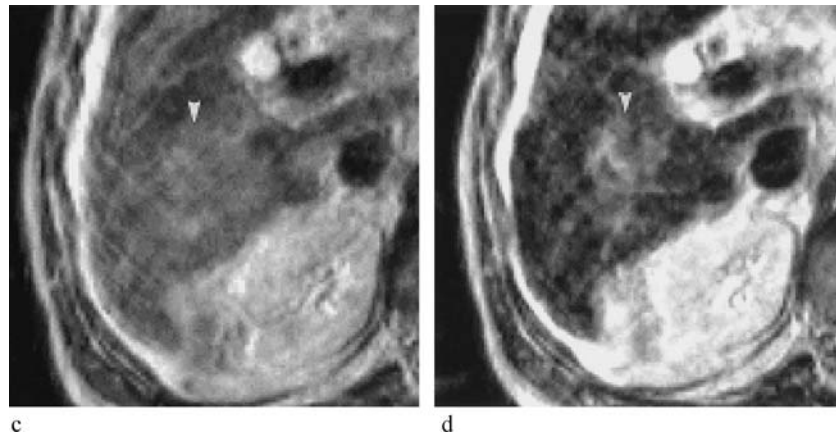
FIGURE 1. Detection of cancer in the liver revealed through SPIO. (C) T2-weighted image without contrast agent indicates the difficulty of determination of lesion. (D) SHU555A enhanced detection in the liver enhanced the conspicuity, leading all readers to rate the signal increase as a definite lesion. Panels (C) and (D) from Fig. 3, in Reimers, 1990.[117]

adults with red marrow hyperplasia. The additional contrast provided by SPIO uptake at and around the pathogenic tissue hypothetically allows for differentiation from hyperplastic marrow. A proposed scheme that parallels Kupffer cell response to SPIO in the liver may be at work; at disease sites SPIO are not taken up by cells in the bone-surrounding epithelial layer.

Macrophage Imaging

The observation that SPIO are efficiently internalized by macrophages and other phagocytic cells has recently led to their evaluation as an MR contrast agent for the diagnosis of inflammatory and degenerative disorders associated with high macrophage phagocytic activity. Applications
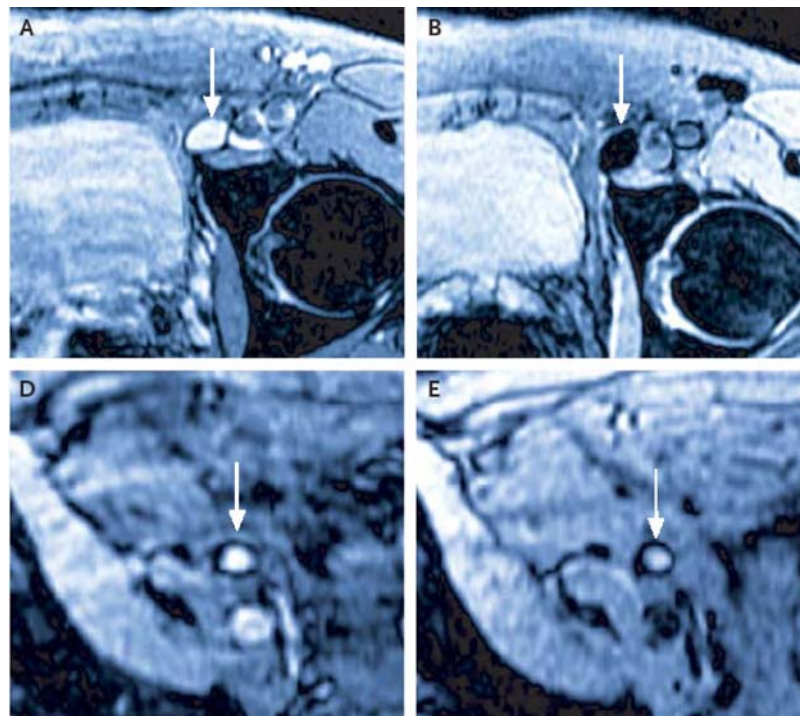

FIGURE 2. The use of intraveneously administered SPIO allows for the differentiation between normal and metastatic lymph nodes. MR images of healthy lymph nodes before (A) and after (B) injection of SPIO shows a homogeneous decrease in the signal. Conversly, MR images of a lymph node filled with a tumor shows a high signal intensity before (D) and after (E) administration of SPIO. Panels (A), (B), (D), and (E) from Fig. 3 in Harsinghani, 2003.[55]

have included identifying sites of transplant rejection[71] and the identification of atherosclerotic plaques.[75,130] Thus far, evidence suggests that macrophage uptake of SPIO at sites of atherosclerosis could indicate disease sites prior to luminal narrowing, leading to earlier diagnosis and treatment.[124] It should be noted that the efficiency of SPIO uptake by macrophage and MR contrast is highly dependent on both circulation time and surface charge.[90] Typically, *in vivo*, smaller nanoparticles (15–30 nm hydrodynamic diameter) with longer circulation times exhibit improved contrast at sites of inflammation compared with larger nanoparticles.[53]

The role of macrophages in pathologic tissue alterations in the central nervous system (CNS) has also provided the opportunity for the use of SPIO agents for the imaging of strokes[127] (Fig. 3), multiple sclerosis,[33] brain tumors,[2,37] and carotid atherosclerotic plaques.[26] In ischemic stroke lesions, the SPIO density and spatial distribution indicates breakdown of the blood–brain barrier. Compartmental release of cytotoxic substances by activated macrophages potentially leads to further CNS damage.[12] In such cases, SPIO-endowed *in vivo* visualization of macrophage activity presents an exciting opportunity to monitor the real-time efficiency of therapeutic intervention. Clean delineation of metastases in the brain was possible through SPIO presence, initially, at the tumor interstitium and, subsequently, through uptake by surrounding tumor cells, approximately 24 h following injection.[37] The definition provided at tumor margins and of single tumor cells surrounding the tumor (micrometastes) highlight the potential of SPIO for use in preoperative planning.

ACTIVE TARGETING

In order to achieve active targeting of SPIO against specific biomolecules, it is necessary to first conjugate targeting agents onto the SPIO surface directly or onto its hydrophilic coating. An advantage of having a polymer coating is that it can usually be modified to possess a variety of reactive moieties (i.e., amines, sulfhydryls, carboxyls, etc.), which subsequently allow for more control over conjugation.

Perhaps the greatest hurdle for active targeting is localizing adequate levels of SPIO at a disease site to generate sufficient contrast for MR detection. With this goal in mind, numerous approaches have been evaluated to effectively enhance MR sensitivity by improving the site-specific accumulation of SPIO. The most widely accepted technique involves intracellular trapping.[72] In this approach, receptor-mediated uptake of SPIO is exploited to accrue elevated levels of the contrast agent within the desired cells.

An alternative approach to improving MR contrast involves a two-step amplification strategy.[8] Specifically, a biotinylated targeting antibody is first introduced intra-venously and is allowed to localize to the specific disease site. Streptavidin-labeled SPIO is then introduced to label each antibody with multiple contrast agents. The avidin–biotin binding system possesses extremely high binding affinity and extension of this technique could be extended to a wide range of targets, although, further development of this targeting method is still required.

Active targeting is preferred to passive targeting since it not only provides physiologic information but also offers insight into specific molecular mechanisms. Such information could allow for the early detection of disease as well as more accurate staging. Numerous studies have already demonstrated the ability of active targeting strategies to identify early markers of cancer and cardiovascular disease, the two leading causes of death.

Cancer Imaging

To date, numerous early markers of cancer have already been evaluated as targets for ligand-directed SPIO. Achievement of satisfactory image contrast generally requires that the targets selected are not only overexpressed specifically on cancer cells, but also undergo receptor-mediated endocytosis upon SPIO binding resulting in intracellular accumulation. One such target is the transferrin receptor, which is overexpressed on a variety of cancer cell types—most notably breast cancer.[142] Numerous studies have shown that SPIO conjugated to transferrin can be used to monitor the expression and regulation of the transferrin receptor *in vitro* and *in vivo*.[60,62,77,94,115]

In parallel to the work with transferrin, SPIO conjugated to folate experienced rapid and effcient uptake by tumor cells overexpressing the folate receptor. *In vivo* MR imaging revealed an average T2 intensity decrease of 38% from pre-contrast to post-contrast images of the tumor.[1,24,138] Another cancer marker recently targeted with SPIO is the underglycosylated MUC-1 tumor antigen (uMUC-1). This antigen is a common feature of numerous epithelial cell adenocarcinomas including breast, pancreatic, colorectal, lung, prostate, and gastric cancers. The antigen was targeted with the peptide EPPT1, which has a known affinity for uMUC-1.[96]

The number of biomarkers that have been targeted with SPIO conjugates for detecting and imaging cancer *in vivo* continues to expand. To name a few; matrix metalloproteinase-2, a membrane-bound endopeptidase found upregulated at gliomas, has been targeted.[69] In this case, the contrast agent consisted of a SPIO–chlorotoxin peptide conjugate.[148] In another embodiment, SPIO–herceptin was able to mark the HEr-2/neu (c-erb B-2) tyrosine kinase receptor.[9,44] This target has been found to be overexpressed on breast cancer cells in 25% of women with metastatic breast cancer. Additionally, a monoclonal antibody bound to SPIO was able to bind an unknown ligand expressed in colorectal cancers.[143]
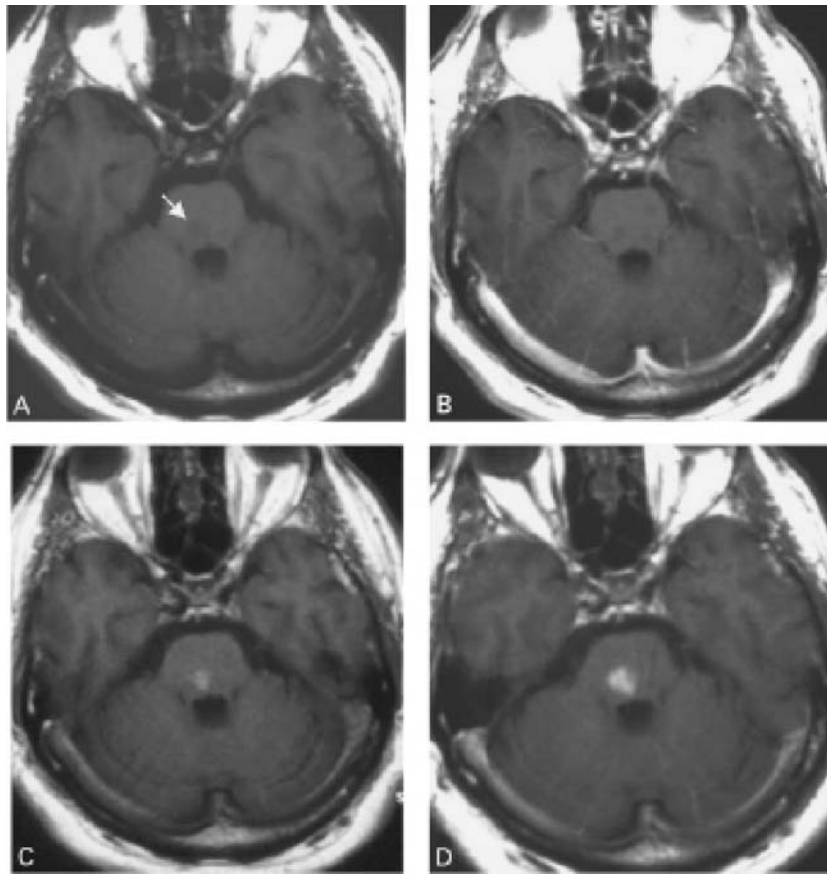
FIGURE 3. Non-enhanced T1-weighted image brainstem infarct (*arrow*) 5 days after stroke (A). A gadolinium contrast agent shows no breach of blood–brain barier (B). Images at 24 h (C) and 48 h (D) following SPIO infusion show amplified signal at infarcted parenchyma (from A. Saleh, 2004,[109]).

An alternative strategy for identifying tumors involves targeting receptors specifically expressed on normal tissues but not tumors. Such a design has been pursued with the CholocystokininA (CCKA) receptor of pancreas acinar cells. CCK is a hormone produced principally by the small intestine in response to the presence of fats that binds to the receptor CCKA. Studies show that upon administration of SPIO–CCK to rats, a significant reduction of T2 relaxation in normal pancreatic tissues but not in tumors was evident, illustrating the feasibility of SPIO-mediated detection of tumors in the pancreas.[120]

The liver is a common site of metastases from a variety of organs including the breasts, lungs, rectum, and colon. Accordingly, much effort has been expended in the research for liver-specific MR contrast agents to characterize liver tumors. It is known that asialoglycoprotein (ASG) receptors are present on normal hepatocytes but are missing in primary malignant or metastatic tumors.[119] To detect liver cancer in rats, SPIO were conjugated to arabinogalactan (AG), a polysacharride that is a ligand of the ASG receptor. MR imaging indicated that the use of AG–SPIO to target normal hepatocytes allows for enhanced tumor–liver contrast.[120]

Imaging Apoptosis

An emerging exploitation of SPIO is the active targeting of cells undergoing apoptosis. Apoptosis plays a role in the pathology of cancer, neurodegeneration, acute myocardial infarction, and chronic inflammation. SPIO targeting apoptotic cells and cues could also allow for the real-time monitoring of drug efficacy. Recently, *in vivo* apoptotic cell detection via MR has been accomplished through the use of the first C2 domain of synaptotagmin I as a targeting moiety.[163] When conjugated to SPIO, significant increases in image contrast were identified in those regions of tumors containing large numbers of apoptotic cells. An alternative method currently being developed for imaging apoptosis involves targeting of the phospholipid phosphatidylserine (PS) with Annexin V.[36] Using Annexin V-conjugated nanoparticles, apoptotic cells could be detected at nanoparticle concentrations as low as 0.1 μg Fe/ml *in vitro*.[128,129]

Cardiovascular Imaging

In addition to cancer and apoptosis, molecular imaging has also taken great strides in improving the contrast and early detection of various cardiovascular diseases
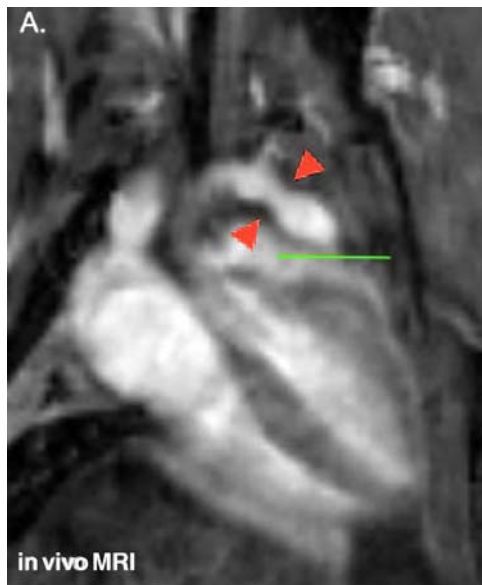
FIGURE 4. MR image of atherosclerotic lesion targeted with SPIO. (A) Following injection of VCAM-1 targeted SPIO into apolipoprotein-deficient mice, clear decreases in signal intensity could be detected in atherosclerotic lesions. Panel (A) from Fig. 6 in Kelly, 2005.[63]

including atherosclerosis, thrombosis, and myocardial infarcts. Detection of early atherosclerotic signatures has recently been performed with anti-VCAM-1 (vascular adhesion molecule-1)-targeted SPIO,[145] as well as SPIO labeled with VCAM-1-specific peptides.[72] In the latter case, phage display was used to identify a VCAM-1-specific cell internalizing peptide. Internalization of the SPIO–peptide conjugates reportedly resulted in a 12-fold higher target-to-background ratio compared with anti-VCAM-1–SPIO conjugates. Through the increased uptake and subsequent compartmental accumulation of SPIO, sites of atherosclerosis were identified in apolipoprotein-deficient mice through the resultant decrease of signal intensity (Fig. 4). Since VCAM-1 has been identified as an early marker for inflammation of the endothelium it is envisioned that these nanoparticles could potentially lead to earlier diagnosis and treatment.

In addition to VCAM-1, E-selectin has also been validated as a potential target for SPIO. E-selectin is a proinflammatory marker of endothelial cells that has been implicated in atherosclerosis, tumor vascular endothelial proliferation, and angiogenesis.[15,23,76] Using SPIO–anti-human E-selectin F(ab′)2 conjugates, E-selectin was detected by MR imaging in human endothelial cell cultures, exhibiting a significant contrast enhancement over control cells.[70]

Imaging of thrombi has recently been accomplished through the specific detection of both αIIb-β3, which is expressed by activated platelets, and activated coagulation factor XIII (FXIIIa), a tissue transglutaminase that cross-links fibrin and plasmin inhibitors to form stable thrombi.[7]

Activated platelets were targeted with SPIO–RGD peptide conjugates in both *ex vivo* and *in vivo* thrombus models.[65] It is well established that RGD, a cyclic arginine-glycine-aspartic acid peptide, specifically targets the αIIb-β3 integrin.[125] SPIO–RGD resulted in better thrombus visualization than non-targeted SPIO *ex vivo*. Furthermore, with MR contrast enhancement, clot visualization *in vivo* was achieved with an in-plane resolution of less than 0.2 mm $\times$ 0.2 mm. FXIIIa was detected *in vivo* using an alpha$_2$AP peptide–SPIO conjugate. Previous reports have demonstrated that alpha$_2$AP peptide is effectively cross-linked by FXIIIa. Results indicated that SPIO–alpha$_2$AP was covalently linked to human plasma thrombi, and MR imaging revealed a marked thrombus contrast enhancement over control agents.[64]

For imaging of myocardial infarcts, antimyosin Fab (R11D10), which are immunospecific to necrotizing myocytes, were conjugated to SPIO. Images showed significant signal decrease of the infarct relative to the surrounding myocardium.[158]

CELL TRACKING

A promising new direction for SPIO is their use in tracking the biodistribution of cells *in vivo*. These studies typically involve implanting SPIO-loaded cells into living subjects and tracking their movement and localization at specific tissues.[43] Various strategies have been employed to efficiently load cultured cells with enough SPIO to ensure sufficient contrast for *in vivo* imaging.[6] Of particular interest is the conjugation of membrane translocating signals such as HIV-Tat and polyArginine peptides to SPIO, which greatly enhance SPIO uptake into many cell types.[68,80] The potential of *in vivo* cell tracking has been demonstrated in several systems including SPIO loaded T cells.[31] Objects as diminutive as single cells were able to be monitored since the T2 relaxation effect of the sequestered magnetic nanoparticles is exerted over a region larger than that of the cell itself. SPIO labeled T cells showed a 20% reduction of signal in the spleen of mice at 3 h post-injection.[30] This correlates with the known pattern of T-cell distribution following injection in mice. The tracking of immune responsive cells, whose activation has been shown to not be impaired in the presence of SPIO,[30] could allow for specific diagnosis and monitoring of treatment.

More recently SPIO has been used to track stem cells upon seeding to a target organ. The distribution of rat mesenchymal stem cells following intravascular injection[16] has been recorded. Non-invasive imaging through T2 drop of the contrast agent was used to track the cells to the kidney and livers of injected rats.

A trimodal (magnetic, fluorescent, isotope) HIV-Tat peptide-labeled CLIO probe was developed and tested[80] in human lymphocytes and hematopoietic cells and in mouse splenocytes and neuronal progenitor cells. The cells were
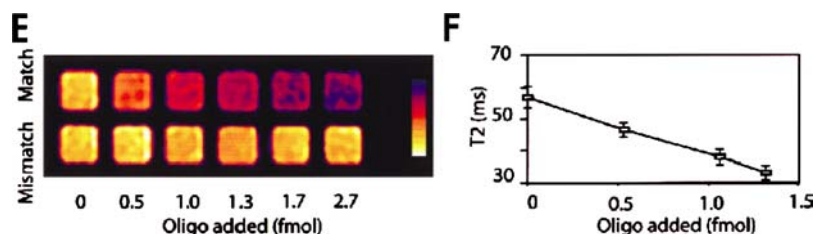
FIGURE 5. Detection of nucleic acids with magnetic relaxation switches (MRS). (E) A color-coded T2-weighted MR image of a 384-well plate with constant amounts of P1 and P2 probes, with varying amounts of matching and mismatched Target. (F) MRI values show the linear drop in T2 correlated to concentration. The sensitivity of the ON MRS nanosensors is robust and sensitive enough to be able to detect extremely low concentrations of probe hybridization. Panels (E) and (F) from Fig. 2 in Perez, 2002.[105]

traceable *in vivo* following implantation in immunodeficient mice, offering detection at the single-cell level.

Internalizing cell surface receptor-mediated endocytosis of SPIO is another avenue through which cell migration can be observed *in vivo*.[27] Bulte and coworkers utilized anti-transferrin receptor antibodies conjugated to nanoparticles in order to observe oligodendrocyte migration post-neurotransplantation.[19] The SPIO did not interfere with the cells' ability to myelinate *in vivo*, and histological evaluation of the cells with nanoparticles revealed cell migration up to 10 mm in 14 days.

MAGNETIC RELAXATION SWITCHING

It has previously been observed that SPIO assemblies undergo a unique magnetic phenomenon, termed magnetic relaxation switching (MRS).[67,105,107,144,164] During this cooperative process, the superparamagnetic iron oxide core of individual nanoparticles become more efficient at dephasing the spins of surrounding water protons, i.e., at enhancing spin–spin relaxation times (T2). Recently, this mechanism has been exploited as a tool for detecting biomolecules in homogeneous assays and has demonstrated detection limits as low as 500 attomoles.[105] Applications have included the detection of oligonucleotides (ON), proteins, enzymes, and enantiomers with very high sensitivity. A major advantage of MRS over many detection schemes is that magnetic changes are detectable in turbid media and whole-cell lysates without the need for protein purification. The tremendous sensitivity of MRS combined with the ability to detect SPIO in deep tissue make MRS a promising approach for *in vivo* applications; although, strategies must still be developed to limit false-positives due to the non-specific aggregation of nanoparticles within endosomes.

Oligonucleotide Detection

The capability of MRS was first demonstrated with the detection of nucleic acids in solution.[67,105] Specifically, two unique SPIO populations were synthesized, where the SPIO-ON constructs were designed to recognize adjacent sites on a nucleic acid target. SPIO self-assembly induced by hybridization to target DNA generated a detectable change in the T2 relaxation time. Conversely, little signal change was detected when SPIO-ON conjugates were introduced to a non-complementary nucleic acid target (Fig. 5). The lower detection limit for this assay was shown to be less than 500 attomoles. Further, the binding occurred within minutes and was reversible. An interesting application of this technique, in a high-throughput screening scheme, is the measurement of telomerase activity, a metric of genetic instability and associated with the formation of malignancies.[49] As little as 10–100 attomoles of target were detected using a benchtop relaxometer. Atomic force microscopy allowed for single molecule detection confirming the SPIO-ON conjugates alignment along target telomeric repeats.

Protein and Enzyme Detection

MRS probes have also been exploited as biosensors capable of detecting specific proteins and even viruses via antibody-mediated interactions.[108] For example, SPIO labeled with surface-specific antibodies raised against adenovirus-5 and herpes simplex virus-1 were used to detect as few as five viral particles per 10 μl via the MRS-based mechanism. A similar detection scheme was also used to detect proteins (e.g., GFP) in cell lysate.[105]

Complementary to MRS assays dependent on the self-assembly of SPIO, assays relying the dispersion of SPIO have also been devised to detect endonuclease, and subsequently, methylase and protease activity.[105,106] Briefly, for endonuclease activity, two sets of SPIO were designed such that attached oligonucleotide sequences hybridized to form a restriction endonuclease recognition site. The T2 relaxation time decreased significantly when the two populations were combined. Subsequent addition of restriction endonucleases resulted in an increase in the T2 relaxation time as the restriction sites were cleaved. This method has also been modified for methylases and proteases by simply switching endonuclease substrates to methylase and protease substrates, respectively.

For MRS assays that are intended for *in vivo* applications, detection strategies that rely on association of

SPIO rather than dissociation are typically preferred to circumvent the problem of glomerular filtration of clustered nanoparticles. Accordingly, MRS sensors for myelperoxidase (MPO), an enzyme associated with atherosclerosis and inflammation,[162] were designed as serotonin-labeled SPIO which become cross-linked in the presence of MPO.[107] Although not validated *in vivo*, these probes certainly take the first steps toward extending MRS-based probes into living subjects.

Enantiomer Detection

Most recently, MRS nanoparticles have been developed to serve as a highly sensitive sensor for enantiomeric impurities.[144] Evidence that considerable differences may be present in the pharmacological activity of certain enantiomers has led to an urgent demand for a system that can detect enantiomeric impurities with high sensitivity, quick execution, and high-throughput capability. To help meet this demand, an MRS-based model system was established where SPIO were first labeled with the enantiomer D-Phe, (SPIO-D-Phe) considered to be the impurity in this case. Antibodies raised against D-Phe were then added to the solution of SPIO-D-Phe resulting in the formation of clusters and a corresponding decrease in the T2 relaxation time. Upon the addition of racemic mixtures of L- and D-Phe, the presence of D-Phe impurities led to the dispersion of the nanoparticles by competing with the SPIO-D-Phe for anti-D-Phe binding sites. This resulted in a detectable increase in the T2 relaxation time. The MRS enantiomeric immunoassay proved capable of detecting enantiomeric impurities at levels far below the requirements of the federal regulatory agencies and also could be adapted to a high-throughput format for pharmaceutical applications.

CONCLUDING REMARKS

The use of MR imaging has become a well-established means for injury and disease diagnosis on the anatomic scale. The search for contrast agents to improve contrast via MR has spurred the development and use of SPIO as a means for imaging not only at the anatomical scale but also the cellular and even molecular level. The intensification of these developments, in the fields of materials science, nanotechnology, and bioconjugation chemistry, has pushed the use of these agents to the boundaries of molecular imaging and beyond. Applications as diverse as cell tracking, gene detection and quantification, molecular interaction, and enzymatic reactions are being observed through the use of SPIO probes.

A motivating advantage for advancing MR as a platform for molecular imaging is that anatomic and molecular information can be gathered simultaneously. Contrarily, a significant drawback of an MR-based approach to molecular imaging is its low sensitivity, particularly compared with nuclear imaging, which has been used to detect probes down to the picomolar level.[110] The inherently low signal-to-noise ratio in MR can be amended through longer scan times, which can become prohibitively long, and the use of stronger magnetic fields. The vast majority of clinical MR units are however at 1.5 T. It should be noted that imaging of individual cells has been accomplished on a clinical scanner with some modifications.[42]

Another limitation of MR-based molecular imaging is the current inability to image more than one biomarker at a time as is commonly performed with optical imaging in combination with contrast agents such as quantum dots. Quantum dots are nanoparticles composed of semiconductor material that are currently in favor thanks to their minimal bleaching (as opposed to fluorophores), a variety of emission wavelengths as controlled by their diameter, and the ability to be conjugated to molecular targeting moieties similar to SPIO (for an introduction, see Gao[45]). Each imaging modality (e.g., MR, optical, nuclear, etc.) clearly exhibits unique advantages and disadvantages when applied to molecular imaging applications and they will undoubtedly continue to compliment each other in the future, particularly with the introduction of new multi-modality imaging platforms.

Effective and innovative imaging approaches are in great demand as new proteins and genes, particularly within the field of oncology, are being discovered at an ever-increasing pace. This provides a constantly multiplying library of molecules and pathways to be studied for prevention, diagnosis, and treatment of diseases. The full potential of new discoveries is however limited by the void between the advances in bioscience and the means to accurately, effectively and—critically—non-invasively image the molecular interactions in biological systems. Many challenges clearly remain in the pursuit of ideal SPIO probes for molecular imaging; increased target affinity, less complex conjugation schemes, reduction of cost, a means for MRS to avoid sequestration in lysosomes and more effective activatable probes. With persistent advances, this system continues to demonstrate its potential as a means to probe deeper into our biological universe.

REFERENCES

[1] Antony, A. C. Folate receptors. *Annu. Rev. Nutr.* 16:501–521, 1996.

[2] Anzai, Y. Superparamagnetic iron oxide nanoparticles: Nodal metastases and beyond. *Top. Magn. Reson. Imaging* 15:103–111, 2004.

[3] Anzai, Y., C. W. Piccoli, E. K. Outwater, W. Stanford, D. A. Bluemke, P. Nurenberg, S. Saini, K. R. Maravilla, D. E. Feldman, U. P. Schmiedl, J. A. Brunberg, I. R. Francis, S. E. Harms, P. M. Som, and C. M. Tempany. Evaluation of neck and body metastases to nodes with ferumoxtran 10-enhanced MR imaging: Phase III safety and efficacy study. *Radiology* 228:777–788, 2003.

[4]Anzai, Y., M. R. Prince, T. L. Chenevert, J. H. Maki, F. Londy, M. London, and S. J. MacLachlan. MR angiography with an ultrasmall superparamagnetic iron oxide blood pool agent. *J. Magn. Reson. Imaging* 7:75–81, 1997.

[5]Arbab, A. S., T. Ichikawa, H. Sou, T. Araki, H. Nakajima, K. Ishigame, T. Yoshikawa, and H. Kumagai. Ferumoxides-enhanced double-echo T2-weighted MR imaging in differentiating metastases from nonsolid benign lesions of the liver. *Radiology* 225:151–158, 2002.

[6]Arbab, A. S., G. T. Yocum, L. B. Wilson, A. Parwana, E. K. Jordan, H. Kalish, and J. A. Frank. Comparison of transfection agents in forming complexes with ferumoxides, cell labeling efficiency, and cellular viability. *Mol. Imaging* 3:24–32, 2004.

[7]Ariens, R. A., T. S. Lai, J. W. Weisel, C. S. Greenberg, and P. J. Grant. Role of factor XIII in fibrin clot formation and effects of genetic polymorphisms. *Blood* 100:743–754, 2002.

[8]Artemov, D., N. Mori, B. Okollie, and Z. M. Bhujwalla. MR molecular imaging of the Her-2/neu receptor in breast cancer cells using targeted iron oxide nanoparticles. *Magn. Reson. Med.* 49:403–408, 2003.

[9]Artemov, D., N. Mori, R. Ravi, and Z. M. Bhujwalla. Magnetic resonance molecular imaging of the HER-2/neu receptor. *Cancer Res.* 63:2723–2727, 2003.

[10]Ayyub, P., M. Multani, M. Barma, V. R. Palkar, and R. Vijayaraghavan. Size-induced structural phase-transitions and hyperfine properties of microcrystalline Fe_2O_3. *J. Phys. C Solid State Phys.* 21:2229–2245, 1988.

[11]Babes, L., B. Denizot, G. Tanguy, J. J. Le Jeune, and P. Jallet. Synthesis of iron oxide nanoparticles used as MRI contrast agents: A parametric study. *J. Colloid Interface Sci.* 212:474–482, 1999.

[12]Banati, R. B., J. Gehrmann, P. Schubert, and G. W. Kreutzberg. Cytotoxicity of microglia. *Glia* 7:111–118, 1993.

[13]Bee, A., R. Massart, and S. Neveu. Synthesis of very fine maghemite particle. *J. Magn. Magn. Mater.* 149:6–9, 1995.

[14]Belin, T., N. Guigue-Millot, T. Caillot, D. Aymes, and J. C. Niepce. Influence of grain size, oxygen stoichiometry, and synthesis conditions on the small gamma, Greek-Fe_2O_3 vacancies ordering and lattice parameters. *J. Solid State Chem.* 163:459–465, 2002.

[15]Bischoff, J., C. Brasel, B. Kraling, and K. Vranovska. E-selectin is upregulated in proliferating endothelial cells *in vitro*. *Microcirculation* 4:279–287, 1997.

[16]Bos, C., Y. Delmas, A. Desmouliere, A. Solanilla, O. Hauger, C. Grosset, I. Dubus, Z. Ivanovic, J. Rosenbaum, P. Charbord, C. Combe, J. W. Bulte, C. T. Moonen, J. Ripoche, and N. Grenier. *In vivo* MR imaging of intravascularly injected magnetically labeled mesenchymal stem cells in rat kidney and liver. *Radiology* 233:781–789, 2004.

[17]Brooks, R. A. T(2)-shortening by strongly magnetized spheres: A chemical exchange model. *Magn. Reson. Med.* 47:388–391, 2002.

[18]Bruckl, H., M. Panhorst, J. Schotter, P. B. Kamp, and A. Becker. Magnetic particles as markers and carriers of biomolecules. *IEE Proc. Nanobiotechnol.* 152:41–46, 2005.

[19]Bulte, J. W., S. Zhang, P. van Gelderen, V. Herynek, E. K. Jordan, I. D. Duncan, J. A. Frank. Neurotransplantation of magnetically labeled oligodendrocyte progenitors: Magnetic resonance tracking of cell migration and myelination. *Proc. Natl. Acad. Sci. USA* 96:15256–15261, 1999.

[20]Carreno, T. G., A. Mifsud, C. J. Serna, and J. M. Palacios. Preparation of homogeneous Zn/Co mixed oxides by spray pyrolysis. *Mater. Chem. Phys.* 27:287–296, 1991.

[21]Caruso, F., M. Spasova, A. Susha, M. Giersig, and R. A. Caruso. Magnetic nanocomposite particles and hollow spheres constructed by a sequential layering approach. *Chem. Mater.* 13:109–116, 2001.

[22]Caruso, F., A. S. Susha, M. Giersig, and H. Mohwald. Magnetic core-shell particles: Preparation of magnetite multilayers on polymer latex microspheres. *Adv. Mater.* 11:950, 1999.

[23]Chapman, P. T., F. Jamar, E. T. Keelan, A. M. Peters, and D. O. Haskard. Use of a radiolabeled monoclonal antibody against E-selectin for imaging of endothelial activation in rheumatoid arthritis. *Arthritis Rheum.* 39:1371–1375, 1996.

[24]Choi, H., S. R. Choi, R. Zhou, H. F. Kung, and I. W. Chen. Iron oxide nanoparticles as magnetic resonance contrast agent for tumor imaging via folate receptor-targeted delivery. *Acad. Radiol.* 11:996–1004, 2004.

[25]Cornell, R. M., and U. Schertmann. The Iron Oxides: Structure, Properties, Reactions, Occurrence and Uses. Weinheim: VCH Publishers, 1996.

[26]Corot, C., K. G. Petry, R. Trivedi, A. Saleh, C. Jonkmanns, J. F. Le Bas, E. Blezer, M. Rausch, B. Brochet, P. Foster-Gareau, D. Baleriaux, S. Gaillard, and V. Dousset. Macrophage imaging in central nervous system and in carotid atherosclerotic plaque using ultrasmall superparamagnetic iron oxide in magnetic resonance imaging. *Invest. Radiol.* 39:619–625, 2004.

[27]Daldrup-Link, H. E., M. Rudelius, R. A. Oostendorp, M. Settles, G. Piontek, S. Metz, H. Rosenbrock, U. Keller, U. Heinzmann, E. J. Rummeny, J. Schlegel, and T. M. Link. Targeting of hematopoietic progenitor cells with MR contrast agents. *Radiology* 228:760–767, 2003.

[28]Decher, G. Fuzzy nanoassemblies: Toward layered polymeric multicomposites. *Science* 277:1232–1237, 1997.

[29]Deng, Y., L. Wang, W. Yang, S. Fu, A. Elaissari. Preparation of magnetic polymeric particles via inverse microemulsion polymerization process. *J. Magn. Magn. Mater.* 257:69–78, 2003.

[30]Dodd, C. H., H. C. Hsu, W. J. Chu, P. Yang, H. G. Zhang, J. D. Mountz Jr., K. Zinn, J. Forder, L. Josephson, R. Weissleder, J. M. Mountz, and J. D. Mountz. Normal T-cell response and *in vivo* magnetic resonance imaging of T cells loaded with HIV transactivator-peptide-derived superparamagnetic nanoparticles. *J. Immunol. Methods* 256:89–105, 2001.

[31]Dodd, S. J., M. Williams, J. P. Suhan, D. S. Williams, A. P. Koretsky, and C. Ho. Detection of single mammalian cells by high-resolution magnetic resonance imaging. *Biophys. J.* 76:103–109, 1999.

[32]Dormer, K., C. Seeney, A. Mamedov, and F. Mondalek. Internalization of nanoparticles in the middle ear epithelium in response to an external magnetic field: Generating a force. Proceedings of Nanotech 2004, 2004.

[33]Dousset, V., C. Delalande, L. Ballarino, B. Quesson, D. Seilhan, M. Coussemacq, E. Thiaudiere, B. Brochet, P. Canioni, and J. M. Caille. *In vivo* macrophage activity imaging in the central nervous system detected by magnetic resonance. *Magn. Reson. Med.* 41:329–333, 1999.

[34]Edelman, R. R. Contrast-enhanced MR imaging of the heart: Overview of the literature. *Radiology* 232:653–668, 2004.

[35]Elliot, S. R. The Physics and Chemistry of Solids. New York: Wiley, 1998.

[36]Emoto, K., N. Toyama-Sorimachi, H. Karasuyama, K. Inoue, and M. Umeda. Exposure of phosphatidylethanolamine on the surface of apoptotic cells. *Exp. Cell Res.* 232:430–434, 1997.

[37]Enochs, W. S., G. Harsh, F. Hochberg, and R. Weissleder. Improved delineation of human brain tumors on MR images using a long-circulating, superparamagnetic iron oxide agent. *J. Magn. Reson. Imaging* 9:228–232, 1999.

[38]Fabry, B., G. N. Maksym, J. P. Butler, M. Glogauer, D. Navajas, and J. J. Fredberg. Scaling the microrheology of living cells. *Phys. Rev. Lett.* 87:148102, 2001.

[39]Fauconnier, N., A. Bee, J. Roger, and J. N. Pons. Synthesis of aqueous magnetic liquids by surface complexation of maghemite nanoparticles. *J. Mol. Liquids* 83:233–242, 1999.

[40]Flacke, S., S. Fischer, M. J. Scott, R. J. Fuhrhop, J. S. Allen, M. McLean, P. Winter, G. A. Sicard, P. J. Gaffney, S. A. Wickline, and G. M. Lanza. Novel MRI contrast agent for molecular imaging of fibrin: Implications for detecting vulnerable plaques. *Circulation* 104:1280–1285, 2001.

[41]Fletcher, F., and E. London. Intravenous iron. *Br. Med. J.* 84, 1954.

[42]Foster-Gareau, P., C. Heyn, A. Alejski, and B. K. Rutt. Imaging single mammalian cells with a 1.5 T clinical MRI scanner. *Magn. Reson. Med.* 49:968–971, 2003.

[43]Frank, J. A., B. R. Miller, A. S. Arbab, H. A. Zywicke, E. K. Jordan, B. K. Lewis, L. H. Bryant Jr., and J. W. Bulte. Clinically applicable labeling of mammalian and stem cells by combining superparamagnetic iron oxides and transfection agents. *Radiology* 228:480–487, 2003.

[44]Funovics, M. A., B. Kapeller, C. Hoeller, H. S. Su, R. Kunstfeld, S. Puig, and K. Macfelda. MR imaging of the her2/neu and 9.2.27 tumor antigens using immunospecific contrast agents. *Magn. Reson. Imaging* 22:843–850, 2004.

[45]Gao, X., L. Yang, J. A. Petros, F. F. Marshall, J. W. Simons, and S. Nie. *In vivo* molecular and cellular imaging with quantum dots. *Curr. Opin. Biotechnol.* 16:63–72, 2005.

[46]Gilchrist, R. K., R. Medal, W. D. Shorey, R. C. Hanselman, J. C. Parrott, and C. B. Taylor. Selective inductive heating of lymph nodes. *Ann. Surg.* 146:596–606, 1957.

[47]Gillis, P., F. Moiny, and R. A. Brooks. On T(2)-shortening by strongly magnetized spheres: A partial refocusing model. *Magn. Reson. Med.* 47:257–263, 2002.

[48]Goodarzi, A., Y. Sayoo, M. T. Swihart, and P. N. Prasad. Aqueous ferrofluid of citric acid coated magnetite particles. *Mater. Res. Soc. Symp. Proc.* 789:129–134, 2004.

[49]Grimm, J., J. M. Perez, L. Josephson, and R. Weissleder. Novel nanosensors for rapid analysis of telomerase activity. *Cancer Res.* 64:639–643, 2004.

[50]Groman, E. V., K. G. Paul, T. B. Frigo, H. H. Bengele, and J. M. Lewis. Heat stable colloidal iron oxides coated with reduced carbohydrates and carbohdrate derivatives, US Patent 6599498, in US, Advanced Magnetics, Inc., 2003.

[51]Gupta, A. Iron infusion into the arterial blood line during haemodialysis: A novel method to remove free iron and reduce oxidative damage. *Nephrol. Dial. Transplant* 15:1482–1484, 2000.

[52]Gupta, A. K., and A. S. Curtis. Surface modified superparamagnetic nanoparticles for drug delivery: Interaction studies with human fibroblasts in culture. *J. Mater. Sci. Mater. Med.* 15:493–496, 2004.

[53]Gupta, A. K., and S. Wells. Surface-modified superparamagnetic nanoparticles for drug delivery: Preparation, characterization, and cytotoxicity studies. *IEEE Trans. Nanobiosci.* 3:66–73, 2004.

[54]Hahn, P. F., D. D. Stark, J. M. Lewis, S. Saini, G. Elizondo, R. Weissleder, C. J. Fretz, and J. T. Ferrucci. First clinical trial of a new superparamagnetic iron oxide for use as an oral gastrointestinal contrast agent in MR imaging. *Radiology* 175:695–700, 1990.

[55]Harisinghani, M. G., J. Barentsz, P. F. Hahn, W. M. Deserno, S. Tabatabaei, C. H. van de Kaa, J. de la Rosette, and R. Weissleder. Noninvasive detection of clinically occult lymph-node metastases in prostate cancer. *N. Engl. J. Med.* 348:2491–2499, 2003.

[56]He, Y. P., S. Q. Wang, C. R. Li, Y. M. Miao, Z. Y. Wu, and B. S. Zou. Synthesis and characterization of functionalized silica-coated Fe_3O_4 superparamagnetic nanocrystals for biological applications. *J. Phys. D Appl. Phys.* 38:1342–1350, 2005.

[57]Herschman, H. R. Molecular imaging: Looking at problems, seeing solutions. *Science* 302:605–608, 2003.

[58]Hinds, K. A., J. M. Hill, E. M. Shapiro, M. O. Laukkanen, A. C. Silva, C. A. Combs, T. R. Varney, R. S. Balaban, A. P. Koretsky, and C. E. Dunbar. Highly efficient endosomal labeling of progenitor and stem cells with large magnetic particles allows magnetic resonance imaging of single cells. *Blood* 102:867–872, 2003.

[59]Hochepied, J. F., and M. P. Pileni. Magnetic properties of mixed cobalt–zinc ferrite nanoparticles. *J. Appl. Phys.* 87:2472–2478, 2000.

[60]Hogemann, D., L. Josephson, R. Weissleder, J. P. Basilion. Improvement of MRI probes to allow efficient detection of gene expression. *Bioconjug. Chem.* 11:941–946, 2000.

[61]Hundt, W., R. Petsch, T. Helmberger, and M. Reiser. Effect of superparamagnetic iron oxide on bone marrow. *Eur. Radiol.* 10:1495–1500, 2000.

[62]Ichikawa, T., D. Hogemann, Y. Saeki, E. Tyminski, K. Terada, R. Weissleder, E. A. Chiocca, and J. P. Basilion. MRI of transgene expression: Correlation to therapeutic gene expression. *Neoplasia* 4:523–530, 2002.

[63]Igartua, M., P. Saulnier, B. Heurtault, B. Pech, J. E. Proust, J. L. Pedraz, and J. P. Benoit. Development and characterization of solid lipid nanoparticles loaded with magnetite. *Int. J. Pharm.* 233:149–157, 2002.

[64]Jaffer, F. A., and R. Weissleder. Seeing within: Molecular imaging of the cardiovascular system. *Circ. Res.* 94:433–445, 2004.

[65]Johansson, L. O., A. Bjornerud, H. K. Ahlstrom, D. L. Ladd, and D. K. Fujii. A targeted contrast agent for magnetic resonance imaging of thrombus: Implications of spatial resolution. *J. Magn. Reson. Imaging* 13:615–618, 2001.

[66]Jolivet, J. P. Metal Oxide Chemistry and Synthesis: From Solutions to Solid State. New York: Wiley, 2000.

[67]Josephson, L., J. M. Perez, and R. Weissleder. Magnetic nanosensors for the detection of oligonucleotide sequences. *Angew Chem. Int. Ed. Engl.* 40:3204, 2001.

[68]Josephson, L., C. H. Tung, A. Moore, and R. Weissleder. High-efficiency intracellular magnetic labeling with novel superparamagnetic-Tat peptide conjugates. *Bioconjug. Chem.* 10:186–191, 1999.

[69]Kachra, Z., E. Beaulieu, L. Delbecchi, N. Mousseau, F. Berthelet, R. Moumdjian, R. Del Maestro, and R. Beliveau. Expression of matrix metalloproteinases and their inhibitors in human brain tumors. *Clin. Exp. Metastasis* 17:555–566, 1999.

[70]Kang, H. W., L. Josephson, A. Petrovsky, R. Weissleder, and A. Bogdanov Jr.. Magnetic resonance imaging of inducible E-selectin expression in human endothelial cell culture. *Bioconjug. Chem.* 13:122–127, 2002.

[71]Kanno, S., Y. J. Wu, P. C. Lee, S. J. Dodd, M. Williams, B. P. Griffith, and C. Ho. Macrophage accumulation associated with rat cardiac allograft rejection detected by magnetic resonance imaging with ultrasmall superparamagnetic iron oxide particles. *Circulation* 104:934–938, 2001.

[72]Kelly, K. A., J. R. Allport, A. Tsourkas, V. R. Shinde-Patil, L. Josephson, and R. Weissleder. Detection of vascular adhesion molecule-1 expression using a novel multimodal nanoparticle. *Circ. Res.* 96:327–336, 2005.

[73]Kemshead, J. T., and J. Ugelstad. Magnetic separation techniques: Their application to medicine. *Mol. Cell. Biochem.* 67:11–18, 1985.

[74]Kim, D. K., W. Voit, W. Zapka, B. Bjelke, M. Muhammed, and K. V. Rao. Biomedical application of ferrofluids containing

magnetite nanoparticles. *Mater. Res. Soc. Symp. Proc.* 676: y8.32.31.31–36, 2001.

[75] Kooi, M. E., V. C. Cappendijk, K. B. Cleutjens, A. G. Kessels, P. J. Kitslaar, M. Borgers, P. M. Frederik, M. J. Daemen, and J. M. van Engelshoven. Accumulation of ultrasmall superparamagnetic particles of iron oxide in human atherosclerotic plaques can be detected by in vivo magnetic resonance imaging. *Circulation* 107:2453–2458, 2003.

[76] Kraling, B. M., M. J. Razon, L. M. Boon, D. Zurakowski, C. Seachord, R. P. Darveau, J. B. Mulliken, C. L. Corless, and J. Bischoff. E-selectin is present in proliferating endothelial cells in human hemangiomas. *Am. J. Pathol.* 148:1181–1191, 1996.

[77] Kresse, M., S. Wagner, D. Pfefferer, R. Lawaczeck, V. Elste, and W. Semmler. Targeting of ultrasmall superparamagnetic iron oxide (USPIO) particles to tumor cells *in vivo* by using transferrin receptor pathways. *Magn. Reson. Med.* 40:236–242, 1998.

[78] LaConte, L. E., N. Nitin, and G. Bao. Magnetic nanoparticle probes. *Mater. Today* 8(Suppl. 1):32–38, 2005.

[79] Lee, S.-J., J.-R. Leong, S.-C. Shin, J.-C. Kim, Y.-H. Chang, Y.-M. Chang, and J.-D. Kim. Nanoparticles of magnetic ferric oxides encapsulated with poly(D,L latide-co-glycolide) and their applications to magnetic resonance imaging contrast agent. *J. Magn. Magn. Mater.* 272–276:2432–2433, 2004.

[80] Lewin, M., N. Carlesso, C. H. Tung, X. W. Tang, D. Cory, D. T. Scadden, and R. Weissleder. Tat peptide-derivatized magnetic nanoparticles allow in vivo tracking and recovery of progenitor cells. *Nat. Biotechnol.* 18:410–414, 2000.

[81] Li, Z., H. Chen, H. B. Bao, and M. Y. Gao. One-pot reaction to synthesize water-soluble magnetite nanocrystals. *Chem. Mater.* 16:1391–1393, 2004.

[82] Lind, K., M. Kresse, N. P. Debus, and R. H. Muller. A novel formulation for superparamagnetic iron oxide (SPIO) particles enhancing MR lymphography: Comparison of physicochemical properties and the in vivo behaviour. *J. Drug Target* 10:221–230, 2002.

[83] London, E. The molecular formula and proposed structure of the iron-dextran complex, imferon. *J. Pharm. Sci.* 93:1838, 2004.

[84] Louie, A. Y., M. M. Huber, E. T. Ahrens, U. Rothbacher, R. Moats, R. E. Jacobs, S. E. Fraser, and T. J. Meade. *In vivo* visualization of gene expression using magnetic resonance imaging. *Nat. Biotechnol.* 18:321–325, 2000.

[85] Lu, Y., B. T. Mayers, and Y. Xia. Modifying the surface properties of superparamagnetic iron oxide nanoparticles through a sol–gel approach. *Nano Lett.* 2:183–186, 2002.

[86] Mack, M. G., J. O. Balzer, R. Straub, K. Eichler, and T. J. Vogl. Superparamagnetic iron oxide-enhanced MR imaging of head and neck lymph nodes. *Radiology* 222:239–244, 2002.

[87] Massart, R. Preparation of aqueous magnetic liquids in alkaline and acidic media. *IEEE Trans. Magn.* 17:1247–1248, 1981.

[88] Massart, R. Magnetic fluids and process for obtaining them, US Patent 4329241, in US, 1982.

[89] Massart, R., E. Dubois, V. Cabuil, and E. Hasmonay Preparation and properties of monodisperse magnetic fluids. *J. Magn. Magn. Mater.* 149:1–5, 1995.

[90] Matuszewski, L., T. Persigehl, A. Wall, W. Schwindt, B. Tombach, M. Fobker, C. Poremba, W. Ebert, W. Heindel, and C. Bremer. Cell tagging with clinically approved iron oxides: Feasibility and effect of lipofection, particle size, and surface coating on labeling efficiency. *Radiology* 235:155–161, 2005.

[91] Moffat, B. A., G. R. Reddy, P. McConville, D. E. Hall, T. L. Chenevert, R. R. Kopelman, M. Philbert, R. Weissleder, A. Rehemtulla, and B. D. Ross. A novel polyacrylamide magnetic

nanoparticle contrast agent for molecular imaging using MRI. *Mol. Imaging* 2:324–332, 2003.

[92] Molday, R. S. Magnetic iron-dextran microspheres, US Patent 4452773, in 1984.

[93] Molday, R. S., and D. MacKenzie. Immunospecific ferromagnetic iron-dextran reagents for the labeling and magnetic separation of cells. *J. Immunol. Methods* 52:353–367, 1982.

[94] Moore, A., J. Basilion, A. Chiocca, and R. Weissleder. Measuring transferrin receptor gene expression by NMR imaging. *Biochim. Biophys. Acta* 1402:239–249, 1998.

[95] Moore, A., E. Marecos, A. Bogdanov Jr., and R. Weissleder. Tumoral distribution of long-circulating dextran-coated iron oxide nanoparticles in a rodent model. *Radiology* 214:568–574, 2000.

[96] Moore, A., Z. Medarova, A. Potthast, and G. Dai. *In vivo* targeting of underglycosylated MUC-1 tumor antigen using a multimodal imaging probe. *Cancer Res.* 64:1821–1827, 2004.

[97] Morais, P. C., P. P. Gravina, A. F. Bakuzis, K. Skeff Neto, and E. C. D. Lima. Magneto-optical properties of ionic magnetic fluids: The effect of the nanoparticle surface passivation. *Phys. Status Solidi C* 1:3575–3578, 2004.

[98] Morales, M. P., S. Veintemillas-Verdaguer, M. I. Montero, and C. J. Serna. Surfance and internal spin canting in γ-Fe$_2$O$_3$ nanoparticles. *Chem. Mater.* 11:3058, 1999.

[99] Morawski, A. M., P. M. Winter, K. C. Crowder, S. D. Caruthers, R. W. Fuhrhop, M. J. Scott, J. D. Robertson, D. R. Abendschein, G. M. Lanza, and S. A. Wickline. Targeted nanoparticles for quantitative imaging of sparse molecular epitopes with MRI. *Magn. Reson. Med.* 51:480–486, 2004.

[100] Mornet, S., S. Vasseur, F. Grasset, and E. Duguet. Magnetic nanoparticles design for medical diagnosis and therapy. *Bioconjug. Chem.* 14:2161–2175, 2004.

[101] Nitin, N., L. E. LaConte, O. Zurkiya, X. Hu, and G. Bao. Functionalization and peptide-based delivery of magnetic nanoparticles as an intracellular MRI contrast agent. *J. Biol. Inorg. Chem.* 9:706–712, 2004.

[102] Palmacci, S., and L. Josephson. Synthesis of polysaccharide covered superparamagnetic oxid colloids, US Patent 5262176, in US, Advanced Magnetics, Inc., 1993.

[103] Papell, S. S. US Patent 3215572, in US, 1965.

[104] Passirani, C., G. Barratt, J. P. Devissaguet, and D. Labarre. Long-circulating nanoparticles bearing heparin or dextran covalently bound to poly(methyl methacrylate). *Pharm. Res.* 15:1046–1050, 1998.

[105] Perez, J. M., L. Josephson, T. O'Loughlin, D. Hogemann, and R. Weissleder. Magnetic relaxation switches capable of sensing molecular interactions. *Nat. Biotechnol.* 20:816–820, 2002.

[106] Perez, J. M., T. O'Loughin, F. J. Simeone, R. Weissleder, and L. Josephson. DNA-based magnetic nanoparticle assembly acts as a magnetic relaxation nanoswitch allowing screening of DNA-cleaving agents. *J. Am. Chem. Soc.* 124:2856–2857, 2002.

[107] Perez, J. M., F. Simeone, A. Tsourkas, L. Josephson, and R. Weissleder. Peroxidase substrate nanosensors for MR imaging. *Nano Lett.* 4:119–122, 2004.

[108] Perez, J. M., F. J. Simeone, Y. Saeki, L. Josephson, and R. Weissleder. Viral-induced self-assembly of magnetic nanoparticles allows the detection of viral particles in biological media. *J. Am. Chem. Soc.* 125:10192–10193, 2003.

[109] Petri-Fink, A., M. Chastellain, L. Juillerat-Jeanneret, A. Ferrari, and H. Hofmann. Development of functionalized superparamagnetic iron oxide nanoparticles for interaction with human cancer cells. *Biomaterials* 26:2685–2694, 2005.

[110] Phelps, M. E. PET: A biological imaging technique. *Neurochem. Res.* 16:929–940, 1991.

[111] Pileni, M. P. Reverse Micelles as Microreactors. *J. Phys. Chem.* 97:6961–6973, 1993.

[112] Pileni, M. P. The role of soft colloidal templates in controlling the size and shape of inorganic nanocrystals. *Nat. Mater.* 2:145–150, 2003.

[113] Pillai, V., P. Kumar, M. J. Hou, P. Ayyub, and D. O. Shah. Preparation of nanoparticles of silver-halides, superconductors and magnetic-materials using water-in-oil microemulsions as nano-reactors. *Adv. Colloid Interface Sci.* 55:241–269, 1995.

[114] Qhobosheane, M., S. Santra, P. Zhang, and W. Tan. Biochemically functionalized silica nanoparticles. *Analyst* 126:1274–1278, 2001.

[115] Qian, Z. M., H. Li, H. Sun, and K. Ho. Targeted drug delivery via the transferrin receptor-mediated endocytosis pathway. *Pharmacol. Rev.* 54:561–587, 2002.

[116] Raynal, I., P. Prigent, S. Peyramaure, A. Najid, C. Rebuzzi, and C. Corot. Macrophage endocytosis of superparamagnetic iron oxide nanoparticles: Mechanisms and comparison of ferumoxides and ferumoxtran-10. *Invest. Radiol.* 39:56–63, 2004.

[117] Reimer, P., N. Jahnke, M. Fiebich, W. Schima, F. Deckers, C. Marx, N. Holzknecht, and S. Saini. Hepatic lesion detection and characterization: Value of nonenhanced MR imaging, superparamagnetic iron oxide-enhanced MR imaging, and spiral CT-ROC analysis. *Radiology* 217:152–158, 2000.

[118] Reimer, P., and P. Landwehr. Non-invasive vascular imaging of peripheral vessels. *Eur. Radiol.* 8:858–872, 1998.

[119] Reimer, P., R. Weissleder, A. S. Lee, J. Wittenberg, and T. J. Brady. Receptor imaging: Application to MR imaging of liver cancer. *Radiology* 177:729–734, 1990.

[120] Reimer, P., R. Weissleder, T. Shen, W. T. Knoefel, and T. J. Brady. Pancreatic receptors: Initial feasibility studies with a targeted contrast agent for MR imaging. *Radiology* 193:527–531, 1994.

[121] Reimers, G. W., and S. E. Khalafalla. Preparing magnetic fluids by a peptizing method. *Bureau Mines Tech. Prog. Rep.* 59, 1972.

[122] Rockenberger, J., E. C. Scher, and A. P. Alivisatos. A new nonhydrolytic single-precursor approach to surfactant-capped nanocrystals of transition metal oxides. *J. Am. Chem. Soc.* 121:11595–11596, 1999.

[123] Rosensweig, R. E. Ferrohydrodynamics. Cambridge: Cambridge University Press, 1985.

[124] Ruehm, S. G., C. Corot, P. Vogt, H. Cristina, and J. F. Debatin. Ultrasmall superparamagnetic iron oxide-enhanced MR imaging of atherosclerotic plaque in hyperlipidemic rabbits. *Acad. Radiol.* 9(Suppl 1):S143–S144, 2002.

[125] Ruoslahti, E. RGD and other recognition sequences for integrins. *Annu. Rev. Cell. Dev. Biol.* 12:697–715, 1996.

[126] Saeed, M., M. F. Wendland, M. Engelbrecht, H. Sakuma, and C. B. Higgins. Value of blood pool contrast agents in magnetic resonance angiography of the pelvis and lower extremities. *Eur. Radiol.* 8:1047–1053, 1998.

[127] Saleh, A., M. Schroeter, C. Jonkmanns, H. P. Hartung, U. Modder, and S. Jander. *In vivo* MRI of brain inflammation in human ischaemic stroke. *Brain* 127:1670–1677, 2004.

[128] Schellenberger, E. A., A. Bogdanov Jr., D. Hogemann, J. Tait, R. Weissleder, and L. Josephson. Annexin V-CLIO: A nanoparticle for detecting apoptosis by MRI. *Mol. Imaging* 1:102–107, 2002.

[129] Schellenberger, E. A., D. Sosnovik, R. Weissleder, and L. Josephson. Magneto/optical annexin V, a multimodal protein. *Bioconjug. Chem.* 15:1062–1067, 2004.

[130] Schmitz, S. A., M. Taupitz, S. Wagner, K. J. Wolf, D. Beyersdorff, and B. Hamm. Magnetic resonance imaging of atherosclerotic plaques using superparamagnetic iron oxide particles. *J. Magn. Reson. Imaging* 14:355–361, 2001.

[131] Schwertmann, U., and R. M. Cornell. Iron Oxides in the Laboratory, Preparation and Characterization. Cambridge: Wiley-VCH, 2003.

[132] Seip, C. T., E. E. Carpenter, C. J. O'Connor, V. T. John, and S. C. Li. Magnetic properties of a series of ferrite nanoparticles synthesized in reverse micelles. *IEEE Trans. Magn.* 34:1111–1113, 1998.

[133] Shamsi, K., T. Balzer, S. Saini, P. R. Ros, R. C. Nelson, E. C. Carter, S. Tollerfield, and H. P. Niendorf. Superparamagnetic iron oxide particles (SH U 555 A): Evaluation of efficacy in three doses for hepatic MR imaging. *Radiology* 206:365–371, 1998.

[134] Shapiro, E. M., S. Skrtic, K. Sharer, J. M. Hill, C. E. Dunbar, and A. P. Koretsky. MRI detection of single particles for cellular imaging. *Proc. Natl. Acad. Sci. USA* 101:10901–10906, 2004.

[135] Shen, T., R. Weissleder, M. Papisov, A. Bogdanov Jr., and T. J. Brady. Monocrystalline iron oxide nanocompounds (MION): Physicochemical properties. *Magn. Reson. Med.* 29:599–604, 1993.

[136] Skold, C. N. Magnetic particles and methods of producing coated magnetic particles, US Patent App. 20020000398, in US, 2002.

[137] Sorensen, C. M. Nanoscale Materials in Chemistry. New York: Wiley, 2001.

[138] Sudimack, J., and R. J. Lee. Targeted drug delivery via the folate receptor. *Adv. Drug Deliv. Rev.* 41:147–162, 2000.

[139] Suslick, K. S., M. M. Fang, and T. Hyeon. Sonochemical synthesis of iron colloids. *J. Am. Chem. Soc.* 118:11960–11961, 1996.

[140] Tanimoto, A., K. Oshio, M. Suematsu, D. Pouliquen, and D. D. Stark. Relaxation effects of clustered particles. *J. Magn. Reson. Imaging* 14:72–77, 2001.

[141] Tebble, R. S., and D. J. Craik. Magnetic Materials. London: Wiley-Interscience, 1969.

[142] Thorstensen, K., and I. Romslo. The transferrin receptor: Its diagnostic value and its potential as therapeutic target. *Scand. J. Clin. Lab. Invest. Suppl.* 215:113–120, 1993.

[143] Toma, A., E. Otsuji, Y. Kuriu, K. Okamoto, D. Ichikawa, A. Hagiwara, H. Ito, T. Nishimura, and H. Yamagishi. Monoclonal antibody A7-superparamagnetic iron oxide as contrast agent of MR imaging of rectal carcinoma. *Br. J. Cancer* 2005.

[144] Tsourkas, A., O. Hofstetter, H. Hofstetter, R. Weissleder, and L. Josephson. Magnetic relaxation switch immunosensors detect enantiomeric impurities. *Angew Chem. Int. Ed. Engl.* 43:2395–2399, 2004.

[145] Tsourkas, A., V. R. Shinde-Patil, K. A. Kelly, P. Patel, A. Wolley, J. R. Allport, and R. Weissleder. *In vivo* imaging of activated endothelium using an anti-VCAM-1 magnetooptical probe. *Bioconjug. Chem.* 16:576–581, 2005.

[146] Vande Berg, B. C., F. E. Lecouvet, J. P. Kanku, J. Jamart, B. E. Van Beers, B. Maldague, and J. Malghem. Ferumoxides-enhanced quantitative magnetic resonance imaging of the normal and abnormal bone marrow: Preliminary assessment. *J. Magn. Reson. Imaging* 9:322–328, 1999.

[147] Veintemillas-Verdaguer, S., M. P. Morales, and C. J. Serna. Effect of the oxidation conditions on the maghemites produced by laser pyrolysis. *Appl. Organometallic Chem.* 15:365–372, 2001.

[148] Veiseh, O., C. Sun, J. Gunn, N. Kohler, P. Gabikian, D. Lee, N. Bhattarai, R. Ellenbogen, R. Sze, A. Hallahan, J. Olson, and M. Zhang. Optical and MRI multifunctional nanoprobe for targeting gliomas. *Nano Lett.* 5:1003–1008, 2005.

[149] Vogl, T. J., R. Hammerstingl, W. Schwarz, M. G. Mack, P. K. Muller, W. Pegios, H. Keck, A. Eibl-Eibesfeldt, J. Hoelzl, B. Woessmer, C. Bergman, and R. Felix. Superparamagnetic iron oxide-enhanced versus gadolinium-enhanced MR imaging for differential diagnosis of focal liver lesions. *Radiology* 198:881–887, 1996.

[150] Wagner, S., J. Schnorr, H. Pilgrimm, B. Hamm, and M. Taupitz. Monomer-coated very small superparamagnetic iron oxide particles as contrast medium for magnetic resonance imaging: Preclinical in vivo characterization. *Invest. Radiol.* 37:167–177, 2002.

[151] Wang, N., J. P. Butler, and D. E. Ingber. Mechanotransduction across the cell surface and through the cytoskeleton. *Science* 260:1124–1127, 1993.

[152] Wang, Y. X., S. M. Hussain, and G. P. Krestin. Superparamagnetic iron oxide contrast agents: Physicochemical characteristics and applications in MR imaging. *Eur. Radiol.* 11:2319–2331, 2001.

[153] Weissleder, R. Monocrystalline iron oxide particles for studying biological tissues, US Patent 5492814, in US, The General Hospital Corporation, 1996.

[154] Weissleder, R., A. Bogdanov, E. A. Neuwelt, and M. Papisov. Long-circulating iron oxides for MR imaging. *Adv. Drug Deliv. Rev.* 16:321–334, 1995.

[155] Weissleder, R., G. Elizondo, J. Wittenberg, A. S. Lee, L. Josephson, and T. J. Brady. Ultrasmall superparamagnetic iron oxide: An intravenous contrast agent for assessing lymph nodes with MR imaging. *Radiology* 175:494–498, 1990.

[156] Weissleder, R., G. Elizondo, J. Wittenberg, C. A. Rabito, H. H. Bengele, and L. Josephson. Ultrasmall superparamagnetic iron oxide: Characterization of a new class of contrast agents for MR imaging. *Radiology* 175:489–493, 1990.

[157] Weissleder, R., P. F. Hahn, D. D. Stark, G. Elizondo, S. Saini, L. E. Todd, J. Wittenberg, and J. T. Ferrucci. Superparamagnetic iron oxide: Enhanced detection of focal splenic tumors with MR imaging. *Radiology* 169:399–403, 1988.

[158] Weissleder, R., A. S. Lee, B. A. Khaw, T. Shen, and T. J. Brady. Antimyosin-labeled monocrystalline iron oxide allows detection of myocardial infarct: MR antibody imaging. *Radiology* 182:381–385, 1992.

[159] Weissleder, R., D. D. Stark, B. L. Engelstad, B. R. Bacon, C. C. Compton, D. L. White, P. Jacobs, and J. Lewis. Superparamagnetic iron oxide: Pharmacokinetics and toxicity. *Am. J. Roentgenol.* 152:167–173, 1989.

[160] Weissleder, R., D. D. Stark, E. J. Rummeny, C. C. Compton, and J. T. Ferrucci. Splenic lymphoma: Ferrite-enhanced MR imaging in rats. *Radiology* 166:423–430, 1988.

[161] Yu, S., and G. M. Chow. Carboxyl group ($-CO_2H$) functionalized ferrimagnetic iron oxide nanoparticles for potential bio-applications. *J. Mater. Chem.* 14:2781–2786, 2004.

[162] Zhang, R., M. L. Brennan, X. Fu, R. J. Aviles, G. L. Pearce, M. S. Penn, E. J. Topol, D. L. Sprecher, and S. L. Hazen. Association between myeloperoxidase levels and risk of coronary artery disease. *JAMA* 286:2136–2142, 2001.

[163] Zhao, M., D. A. Beauregard, L. Loizou, B. Davletov, and K. M. Brindle. Non-invasive detection of apoptosis using magnetic resonance imaging and a targeted contrast agent. *Nat. Med.* 7:1241–1244, 2001.

[164] Zhao, M., L. Josephson, Y. Tang, and R. Weissleder. Magnetic sensors for protease assays. *Angew Chem. Int. Ed. Engl.* 42:1375–1378, 2003.

[165] Zimmer, C., R. Weissleder, K. Poss, A. Bogdanova, S. C. Wright Jr., and W. S. Enochs. MR imaging of phagocytosis in experimental gliomas. *Radiology* 197:533–538, 1995.